Controlled Drug Release from Porous Polyelectrolyte Multilayers

Michael C. Berg,[†] Lei Zhai,[‡] Robert E. Cohen,*[,†] and Michael F. Rubner*[,‡]

Departments of Chemical Engineering and Materials Science and Engineering, Massachusetts Institute of Technology, Cambridge, Massachusetts 02139

Received March 7, 2005; Revised Manuscript Received June 9, 2005

Microporous and nanoporous polyelectrolyte multilayer films have been explored as ultrathin coatings for controlled drug release. Ketoprofen and cytochalasin D were successfully loaded into nanoporous films and showed zero-order release kinetics over a period of many days. In addition to homogeneous porous multilayers, heterostructures comprising porous regions stacked alternately with nonporous regions were assembled. The heterostructures behaved as dielectric mirrors, which made it possible to optically monitor the loading process. The effects of varying the number of layers in porous and nonporous regions as well as the pore size on the drug release properties were studied. Nonporous regions in the film had no effect on the release rate or duration of release. The amount of drug released could be tuned by varying the number of layers in the porous regions of films, and the release rate depended on the pore size in the films. Microporous multilayers exhibited a Fickian diffusion of drug that was approximately twice as fast as the corresponding nanoporous films. Finally, cell culture experiments with WT NR6 fibroblasts confirmed that cytochalasin D retained its ability to inhibit mitosis after release from the multilayers.

Introduction

Controlled drug release materials have potential for utilization in biomedical implants, tissue engineering, and targeted drug delivery devices. The advantages of controlled release include greater drug effectiveness, better balanced drug concentrations in the body, and more convenience to the patient.[1] In addition, when the drug releasing agents are targeted for specific cell types or applied to an implant surface, they offer a means for local delivery, which reduces toxicity and increases the efficiency of the drug. One example of a drug releasing implant is a drug-eluting coronary stent for possible prevention of restenosis. Restenosis is a deleterious process that results in the narrowing or closing of an artery after some cardiac surgeries. In this application, coatings that elute a variety of drugs including anticoagulants, corticosteroids, and antimitotic agents have been employed.[2,3] Porous materials offer a means to load such drugs and perhaps better control their release. The porous polyelectrolyte multilayers discussed in this paper can be designed to provide sustained release at a specified rate for a selected period of time, and therefore offer very promising properties as stent coatings as well as many other biomedical applications. In fact, one of the drugs studied, cytochalasin D, has been investigated for possible prevention of restenosis[4] due to its ability to block contraction of microfilaments and subsequent effect on cell division and motility.

Over the past decade, polyelectrolyte multilayers have shown a great deal of promise due to the high degree of control over film properties, flexibility in choice of assembly components, and ease of processing possible with these layer-by-layer assembled thin films. Polyelectrolyte multilayers are ultrathin films, which are assembled one molecular layer at a time by taking advantage of attractive interactions between the constituents.[5] These films have shown potential in the area of biomaterials with particular applications in controlled cell−surface interactions,[6−10] cell arrays,[11] drug delivery,[12−20] and biosensors.[21] In the area of drug delivery, polyelectrolyte multilayers coated onto drug microparticles have been shown to prolong the release time of the drug.[13,22] The permeability of the drug through the multilayer coating could be controlled through changes in the number of layers and the polymers used during multilayer assembly. However, the maximum release time achieved was only on the order of hours when using the multilayer films as barriers. Longer release times have been achieved using thermoresponsive multilayers containing poly(*N*-isopropylacrylamide-*co*-acrylic acid) to deliver such drugs as insulin[18] and doxorubicin.[19] Another promising approach is degradable polyelectrolyte multilayers, which have been studied for releasing DNA[23] or charged polymer drugs such as heparin.[24] In this case, the films were built by alternating the selected drug with polyelectrolytes containing hydrolytically degradable ester bonds. A linear release profile was generated as the layers degraded and the drug could escape. Linear release means the rate of drug release remains constant over time, which is a very desirable attribute because it leads to a consistent drug concentration in a patient's body. Polyelectrolyte multilayers have also been examined as drug delivery coatings specifically engineered for stents.[25] In this case, sodium nitropusside was loaded into the multilayers during the polycation assembly steps.

Our approach with polyelectrolyte multilayers is very different. Instead of using the films as barriers to release or as degradable films, we utilized porous weak polyelectrolyte multilayers as micro- or nanoscale containers for holding and releasing the drug. A similar strategy for controlled release has been used for porous silicon,[26,27] which is capable of sustained release of drug molecules over the course of hours to a few days. However, there are many distinct advantages to polyelectrolyte multilayers. Besides their ability to coat virtually any substrate, the key parameters of weak polyelectrolyte multilayers such as bilayer thickness and composition can be modified

* Corresponding authors. E-mail: recohen@mit.edu (R.E.C.); rubner@mit.edu (M.F.R.).

[†] Department of Chemical Engineering.

[‡] Department of Materials Science and Engineering.

10.1021/bm050174e CCC: $33.50
Published on Web 12/17/2005

Table 1. Thickness of Multilayer Films before and after Porosity Transition and Thickness Increase Due to Porosity Induction[a]

	notation	thickness w/o pores (nm)	thickness w/ pores (nm)	thickness increase (nm)
$(PAH/PAA)_8$ NP	8NP	101	253	153
$(PAH/PAA)_{15}$ NP	15NP	202	373	171
$(PAH/PAA)_{20}$ NP	20NP	296	476	180
$(PAH/SPS)_{50.5}$–$(PAA/PAH)_5$–$(SPS/PAH)_{50}$ NP	50-5NP-50	251	327	77.5
$(PAH/SPS)_{50.5}$–$(PAA/PAH)_8$–$(SPS/PAH)_{50}$ NP	50-8NP-50	296	391	95.7
$(PAH/SPS)_{50.5}$–$(PAA/PAH)_8$–$(SPS/PAH)_{130}$ NP	50-8NP-13 0	494	577	83.4
$(PAH/SPS)_{50.5}$–$[(PAA/PAH)_5$–$(SPS/PAH)_{50}]_3$ NP	50-3(5NP-50)	551	688	137
$(PAH/PAA)_{15}$ MP	15MP	202	521	320
$(PAH/PAA)_{20}$ MP	20MP	296	625	329

[a] NP designates nanoporous films, and MP designates microporous films.

through simple pH adjustment during assembly.[28] Also, polymers provide a better means to mimic biological materials as compared to silicon. Mendelsohn et al.[29] were the first to demonstrate a porosity transition in certain multilayers made from the weak polyelectrolytes, poly(allylamine hydrochloride) (PAH) and poly(acrylic acid) (PAA). Since that time, these porous films have been suggested for use in many optical applications such as antireflection coatings,[30] Bragg reflectors,[31] and optical shutters.[32] In this work, we present data indicating that these pores can be loaded with small molecule drugs for controlled release in a buffer solution. Specifically, ketoprofen, a common antiinflammatory drug, and cytochalasin D, a cell division inhibitor, were studied as model drugs. Polyelectrolyte multilayers loaded with charged drugs have previously demonstrated controlled release into aqueous solutions,[15,17] but the films released small molecules very quickly in a buffer solution.[15] In contrast, porous PAH/PAA multilayers extend the total release time to many days in buffer. In addition, by changing the number of layers and pore size, the release duration and rate can be controlled. Finally, we show that multilayer heterostructures composed of alternating porous and nonporous regions act as dielectric mirrors that allow the drug loading process to be monitored optically.

Experimental Section

Materials. Poly(acrylic acid) (PAA) (MW = 90 000; 25% aqueous solution) was purchased from Polysciences. Poly(allylamine hydrochloride) (PAH) (MW = 70 000), poly(sodium 4-styrene-sulfonate) (SPS) (MW = 70 000), cytochalasin D, and ketoprofen were purchased from Sigma-Aldrich. Dulbecco's Phosphate Buffered Saline (PBS) solution was obtained from Gibco/Invitrogen. All materials were used without any further purification.

Substrate Preparation. As described previously,[33] polyelectrolyte multilayer films were assembled using a layer-by-layer dipping technique. The dipping process was automated by an HMS programmable slide stainer from Zeiss, Inc. Dilute polyelectrolyte solutions were prepared (10^{-2} M based on repeat unit of the polymer) with 18 MΩ Millipore water and were pH-adjusted with HCl or NaOH. PAH/PAA multilayers were built by alternately adsorbing PAH (pH = 8.5) and PAA (pH = 3.5) from 10^{-2} M aqueous solutions for 15 min onto a glass microscope slide or a PAH/SPS block. Between polymer solutions, the substrate was taken through a series of three rinse baths of 18 MΩ Millipore water for 2, 1, and 1 min, respectively. This procedure was repeated until either 5, 8, 15, or 20 bilayers were built. A bilayer is defined as a layer of polycation and polyanion. PAH/SPS multilayers were assembled using 10^{-2} M aqueous solutions of PAH (pH = 4.0) and SPS (pH = 4.0) with 0.1 M NaCl added to the solutions. For these blocks, the substrate was immersed for 5 min in the polyelectrolyte solutions followed by the same rinsing procedure described above. The PAH/SPS blocks contained either 50, 50.5, or 130 bilayers.

The multilayer films were assembled to contain either a single porous PAH/PAA region or an architecture composed of PAH/PAA and PAH/SPS alternating blocks. For films containing both types of blocks, a 50.5 bilayer block of PAH/SPS was assembled first, followed by alternating blocks of PAH/PAA and PAH/SPS with PAH/SPS left as the last block. The designations for all of the films fabricated are presented in Table 1, where, for example, $(PAH/PAA)_{15}$ corresponds to 15 bilayers of PAH/PAA.

Porosity Induction. The assembled polyelectrolyte multilayer films were immersed in pH 2.0, 2.2, or 2.3 water for 5 min followed by treatment in pH 5.5 (DI water) or pH 10.0 NaOH solution for 5 min. This sequential process creates either nanoporous or microporous films depending on the pH treatment as previously described.[29,31] After the porosity transition, the films were then heated at 180 °C for 2 h to cross-link the films and lock in the porous structure.

Drug Loading and Release. The model drugs, ketoprofen and cytochalasin D, were loaded into the porous multilayer films through either absorption or by wicking from a DMSO solution. For films loaded using absorption, the multilayers were immersed in the drug solution for 8 h. The wicking experiments were carried out by placing the edge of the multilayer film into the drug solution and allowing the drug solution to wick up the film for 8 h. Films were then rinsed in phosphate buffered saline (PBS) for 2 h to displace the DMSO and eliminate any loosely bound drug. When DMSO filled the pores in the films, the reflectivity changed drastically, so, this phenomenon could be used to monitor the drug loading the pores and removal of DMSO during rinsing. After rinsing, samples were submerged in PBS, and the release of the drug was then monitored using a Cary 6000i UV−vis NIR spectrophotometer from Varian. An aliquot was taken from the PBS solution (in which the sample was submerged), and the absorbance peak height of the aliquot was measured at 260 nm for ketoprofen or 280 nm for cytochalasin D. Finally, the aliquot was returned to the sample container. The absorbance values were translated to concentra-

tion values by comparing to standard solutions for each drug. Standard solutions were prepared in PBS ranging in concentration from 10 to 1000 ng/mL, and the applicability of Beers Law was confirmed for the absorbance values obtained in the drug release studies. After converting the absorbance peak heights to concentration values, they were plotted versus time until a plateau was reached and persisted for at least 10 days. The total amount of drug released from the films was obtained from the value of drug concentration in the plateau region of the graph, and the time at which the plateau first developed was the total release time. For nanoporous films, in which the release curve was linear, the release flux could be obtained from the slope of a line fitted to the data.

Cell Culture. Murine wild type (WT) NR6 fibroblasts were provided by Prof. Linda Griffith's laboratory at MIT for the cell culture experiments. These fibroblasts are a cell line derived from NIH 3T3 cells. Unless noted otherwise, all materials used for cell culture were purchased from Gibco/Invitrogen. The substrates coated with cytochalasin D loaded multilayer films were sterilized by treatment with 70% (v/v) ethanol. As studied in previous work,[9] the sterilization procedure does not change the properties of the multilayer films. The WT NR6 fibroblasts were cultured in pH = 7.4 media comprised of Modified Eagles Medium-α (MEM-α) with 7.5% (v/v) fetal bovine serum (FBS), 1% (v/v) sodium pyruvate (100 mM), 1% (v/v) nonessential amino acids (10 mM), 1% (v/v) Geneticin (G418) antibiotic (350 μg/10 mL PBS), 1% (v/v) L-glutamine (200 mM), 1% (v/v) penicillin (10 000 U/mL, from Sigma), and 1% streptomycin (10 mg/mL, from Sigma). Cells were kept in a humid incubator at 37.5 °C and 5% CO_2.

For cell assays, WT NR6 fibroblasts were counted using a hemocytometer with trypan blue exclusion for cell viability, and seeded at ~10 000 cells/cm^2 onto the substrates. Micrographs documenting cell growth, spreading, and morphology were taken using a Nikon Eclipse TE300 inverted phase contrast microscope with Openlab 3.0 software.

DAPI Staining. After the WT NR6 fibroblasts were on either the control or the cytochalasin D releasing surfaces for 3 days, the nuclei were stained with 4′,6-diamidino-2-phenylindole dihydrochloride (DAPI) to elucidate the effects of cytochalasin D. All products were purchased from Sigma-Aldrich, and dilutions were made in PBS. Cells were fixed with 3.7% formaldehyde solution and made permeable with 0.1% Triton X-100. The nuclei were then stained with 0.5 μg/mL DAPI solution for 15 min. A Zeiss Axioplan 2 fluorescence microscope (Carl Zeiss Inc., Thornwood, NY) with a high-resolution digital camera was used to take pictures of the stained samples.

Film Characterization. Dry film thicknesses were obtained using a Tencor P-10 Surface Profiler (Tencor, Santa Clara, CA). Each data point presented represents an average of at least three independent measurements. The error for profilometry was approximately 3%. The Digital Instruments Dimension 3000 atomic force microscope (AFM) (Digital Instruments, Santa Barbara, CA) was used in tapping mode to obtain topographical information about the film surface including average pore sizes and range in pore size.

Statistical Analysis. Analysis of variance (ANOVA) was used to test the statistical significance of release rate and amount released for the samples. ANOVA determines whether the variance in drug release between different multilayer architectures is greater than the variance within samples of the same multilayer architecture. A *p*-value (or probability value) of the ANOVA test that is less than 0.05 means the drug release properties are statistically different (based on a 5% confidence level).

Results and Discussion

Porous Film Characterization. In this study, two types of polyelectrolyte multilayer architectures were examined. These included multilayer films with only a single porous region, and heterostructure films containing both porous and nonporous regions. Previous work demonstrated that structures with alternating porous and nonporous regions behave as dielectric mirrors due to the difference in the indices of refraction of the different regions and that these porous heterostructures could be loaded with small molecules such as liquid crystals.[31] Both types of multilayer films were loaded with either ketoprofen or cytochalasin D. In addition to these materials, we have successfully loaded and released progesterone, indomethacin, camptothecin, and β-estradiol from nanoporous multilayers. Ketoprofen and cytochalasin D were selected from this group to study in detail; their chemical structures are shown in Figure 1. Cytochalasin D prevents cells from undergoing mitosis (discussed in detail in a later section) and therefore was used as a marker to prove that a drug released from a porous multilayer remains functional. Ketoprofen is an interesting drug because in neutral to high pH environments, the acid group loses its proton and becomes charged and relatively hydrophilic.[34] Ketoprofen and cytochalasin D were each dissolved in DMSO and loaded into the films using two methods: absorption and wicking. In the absorption process, the whole film was submerged in the drug solution, whereas only the edge of the film was brought into contact with the drug solution in the wicking method. By creating films that behave as dielectric mirrors, it was possible to monitor the wicking process through the change in reflectivity that occurs as the pores were filled with the DMSO solution during loading. This phenomenon will be discussed in detail later.

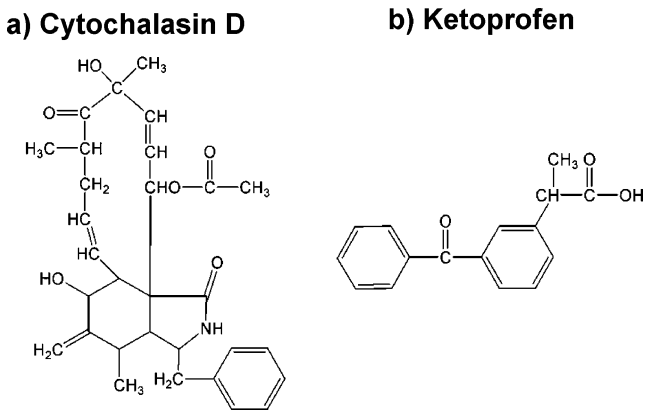

Figure 1. Chemical structures of (a) cytochalasin D and (b) ketoprofen.

Due to the molecular level control over assembly, many different parameters can be tuned in the multilayer heterostructures including the number of porous bilayers, number of nonporous bilayers, the arrangement of the porous bilayers (one region in the middle or several regions throughout the film), and the pore size (controlled post-assembly). Nine different architectures of polyelectrolyte multilayers were prepared to examine the effect that varying these parameters had on the drug release properties. Table 1 lists the different polyelectrolyte multilayers assembled, the dry film thicknesses before and after porosity induction, and the notation used for each film. There were three basic structures incorporated in this study. First, films were assembled that contained only porous PAH/PAA multilayers. These films are designated as 8NP, 15NP, 20NP, 15MP, and 20MP. In the notation, *y*NP or *y*MP, *y* refers to the number of porous PAH/PAA bilayers, and NP or MP is short for nanopores or micropores, respectively. The second basic structure examined was a sandwich structure (50-5NP-50, 50-8NP-50, 50-8NP-130) comprised of a porous region between nonporous regions. In the nomenclature, *x*-*y*NP-*z*, *x* is the number of nonporous PAH/SPS bilayers (nomenclature truncated to 50 from 50.5) nearest the substrate, *y* is the number of nanoporous PAH/PAA bilayers in the middle of the sandwich

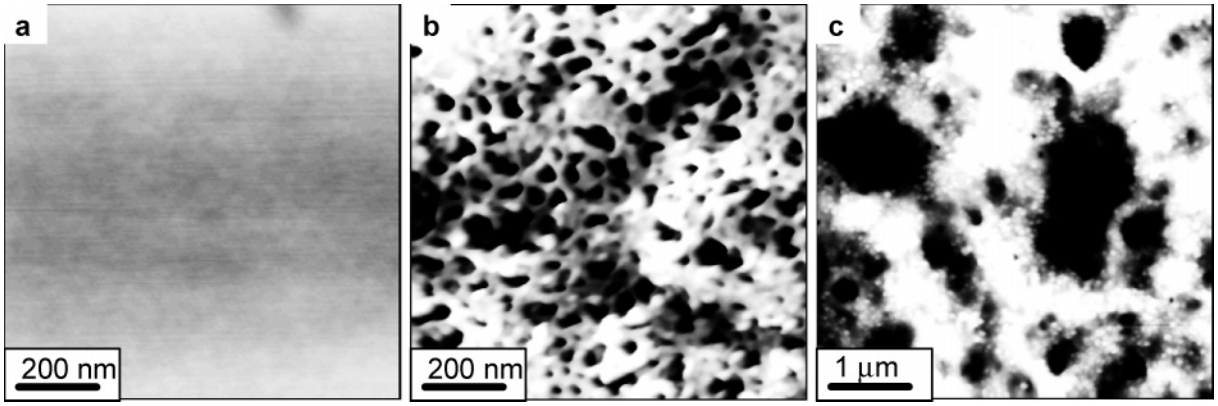

Figure 2. AFM images of (a) nonporous (image size = 1 × 1 μm), (b) nanoporous (image size = 1 × 1 μm), and (c) microporous (image size = 5 × 5 μm) 20 bilayer PAH/PAA multilayer films.

structure, and *z* is the number of nonporous PAH/SPS bilayers in the outermost region of the film. Finally, one multilayer film was built in a multi-stack architecture (50-3(5NP-50)) containing seven alternating nonporous and nanoporous regions. The region closest to the substrate contained 50.5 nonporous PAH/SPS bilayers. The other six regions were alternating nanoporous regions composed of 5 PAH/PAA bilayers and nonporous regions composed of 50 PAH/SPS bilayers. This configuration left PAH/SPS layers as the outermost region of the film.

The nanoporous films had an average pore diameter of 100 nm, and the pores ranged in diameter from approximately 10 to 150 nm (obtained through AFM and SEM, data not shown). The microporous films had pores ranging in diameter from approximately 300 nm to 2 μm with an average pore diameter of 1.0 μm. As shown in Table 1, the increase in film thickness due to the introduction of pores depended greatly on the architecture of the film. In general, thicker multilayers showed a smaller percentage increase in thickness after the porosity induction. In addition, the introduction of nonporous regions further reduced the change in thickness resulting from pore formation. Details concerning the origin of this behavior have been previously reported.[31] Figure 2 shows AFM images of nonporous, nanoporous, and microporous 20 bilayer PAH/PAA films as examples of the surface morphology. These images are typical of the film morphology observed in these three cases.

Loading and Releasing Drugs. Both absorption and wicking from DMSO solutions provided efficient loading of ketoprofen and cytochalasin D. The wicking technique involved dipping one end of the film into the drug solution and allowing the liquid to wick up the film. Drug solutions only wicked into the porous regions when the films had a sandwich or stacked structure. Without the nonporous layers on the outside of the film, a capillary effect would not be established because there would not be the boundary surface needed to provide an interfacial force on the solution. Thus, it was necessary to load the 8NP, 15NP, 20NP, 15MP, and 20MP films by the absorbance method. The wicking technique was developed in previous work, where it was shown that liquid crystals or ionic liquids could be successfully loaded into both nanoporous[31] and microporous[32] polyelectrolyte multilayers with outermost nonporous regions. As mentioned earlier, the wicking front could be observed by the change in reflectivity of the polyelectrolyte multilayer films as the DMSO solution filled the pores. Figure 3 demonstrates this principle by showing a 50-3(5NP-50) multilayer film being loaded with 0.2 mg/mL cytochalasin D in DMSO. The change in color halfway up the film is due to the drug solution filling the pores and changing the film's reflectivity. The wicking process took less than an hour, but films were left for 8 h in the drug solution for convenience. Films were also loaded with drugs by submerging the entire film into the drug solution and allowing it to absorb for 8 h. This method allows the use of nonplanar substrates and films without nonporous regions. Similar results were obtained from both loading techniques as long as the samples were thoroughly rinsed after the loading step. As a control, we attempted to load drugs into sandwich structured films with closed pores using both loading techniques. The wicking process was unsuccessful for these controls, and when drugs were absorbed into the films, the entire amount released in a few minutes during the rinse step. These control experiments indicate that open pores in the multilayers are essential for loading and controlled release of these particular drugs. To simplify matters, all data in the remainder of this paper were obtained from samples loaded via the absorption loading technique because it could be applied to all of the film architectures.

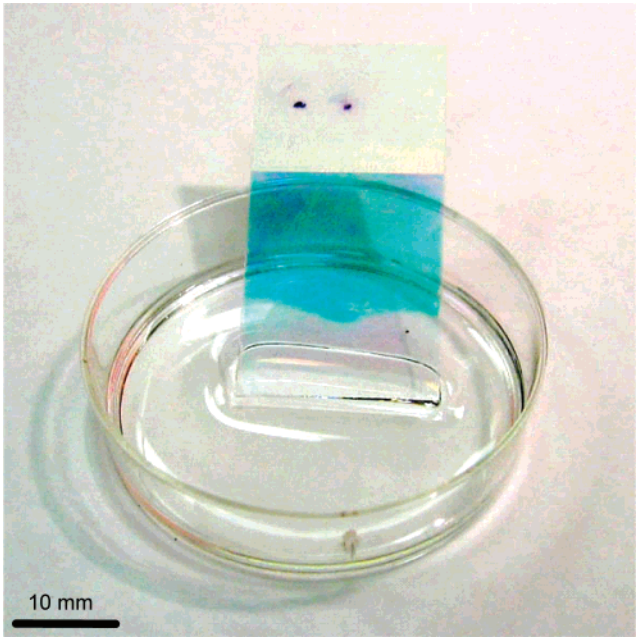

Figure 3. A DMSO solution containing 0.2 mg/mL cytochalasin D in the process of wicking into a 50-3(5NP-50) polyelectrolyte multilayer film. The change in reflectivity halfway up the film is due to the pores being filled with solution.

Drug-loaded samples were rinsed for 2 h in PBS to remove loosely bound drug and to displace DMSO. After rinsing and drying the porous multilayers, the reflectivity of the loaded (but DMSO-free) multilayers returned to essentially the same value

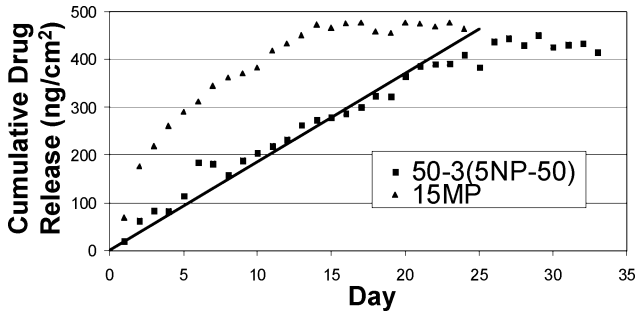

Figure 4. Plot of the cumulative amount of cytochalasin D released from 50-3(5NP-50) and 15MP films as a function of time (drug loaded from a 0.2 mg/mL DMSO solution in both cases).

observed before the loading process. The amount of drug loaded into the pores was therefore too small to affect the films' optical properties. This suggests that the drug does not fill the pores, but only coats the pore walls. Figure 4 displays the drug release results from 50-3(5NP-50) and 15MP films as examples of typical release profiles for a nanoporous and a microporous film, respectively. All nanoporous samples displayed zero-order release kinetics (constant slope on an amount released versus time plot) for nearly the entire time of the experiment. The deviation from zero-order kinetics in the last day or two results from the drug nearing total depletion. In contrast, the microporous films showed a release behavior that was far from linear (R^2 values obtained from fitting a line ranged from 0.5 to 0.6), as shown in Figure 4. The differences between these two release behaviors will be discussed in detail in a later section.

For both nanoporous and microporous films, the samples were monitored for 10 days after the drug concentration in the PBS release solution reached a constant value. To determine if the build-up of drug concentration in the PBS release solution affected the total amount of drug released, each sample was placed in fresh PBS and monitored for 5 additional days following the above-mentioned protocol. No more drug eluted, indicating that the drug concentration in solution did not influence the endpoint of release.

To study the effect of drug concentration in the DMSO loading solution, two different concentrations of each drug were used for a subset of nanoporous films. For ketoprofen, 0.2 and 10.0 mg/mL concentrations were examined, and for cytochalasin D, 0.2 and 1.0 mg/mL concentrations. Figure 5 shows that for all film architectures, the loading concentration had little effect on the total release time or release rate; the values of these parameters increased slightly with an increased drug loading concentration, but most of the results were not statistically different. These results indicate that the amount of drug adsorbed to or coated on the pore walls is unaffected by the loading concentration. In other words, the ultrathin coating of drug on the pore walls appears to be self-limiting.

Table 2. Release Data for Each Film and Drug Tested at a Drug Loading Concentration of 0.2 mg/mL

film	drug	total release time (days)	release flux (ng/cm²/day)	total amount released[a] (ng/cm²)
8NP	ketoprofen	7.8	28.2[b]	219
	cytochalasin D	11.9	23.1	275
15NP	ketoprofen	15.6	22.8	356
	cytochalasin D	24.3	17.2	418
20NP	ketoprofen	18.4	22.0	405
	cytochalasin D	33.9	16.0	543
50-5NP-50	ketoprofen	4.5	25.8	116
	cytochalasin D	7.8	20.3	158
50-8NP-50	ketoprofen	8.0	27.8	223
	cytochalasin D	11.6	22.3	259
50-8NP-130	ketoprofen	7.5	27.7	209
	cytochalasin D	11.0	22.1	243
50-3(5NP-50)	ketoprofen	11.9	26.8	319
	cytochalasin D	22.3	19.5	435
15MP	ketoprofen	6.0	50.7[c]	304
	cytochalasin D	14.0	33.6	471
20MP	ketoprofen	7.5	48.0	360
	cytochalasin D	16.0	32.3	517

[a] Total amount released is approximately equal to the amount loaded after rinsing for all films. [b] For all NP films, the release flux was independent of time. [c] The reported values of release flux for MP films are effective mean values obtained by dividing the total amount of drug released by the total release time.

Table 2 summarizes the release data for the multilayer films examined in this study with a loading concentration of 0.2 mg/mL for both ketoprofen and cytochalasin D. The release data represent values averaged over the entire multilayer coating and are therefore expressed per unit film area (for example, total amount released from a coated microscope slide divided by the actual film area). The multilayers in Table 2 were chosen to illustrate the effects of various key structural parameters on the

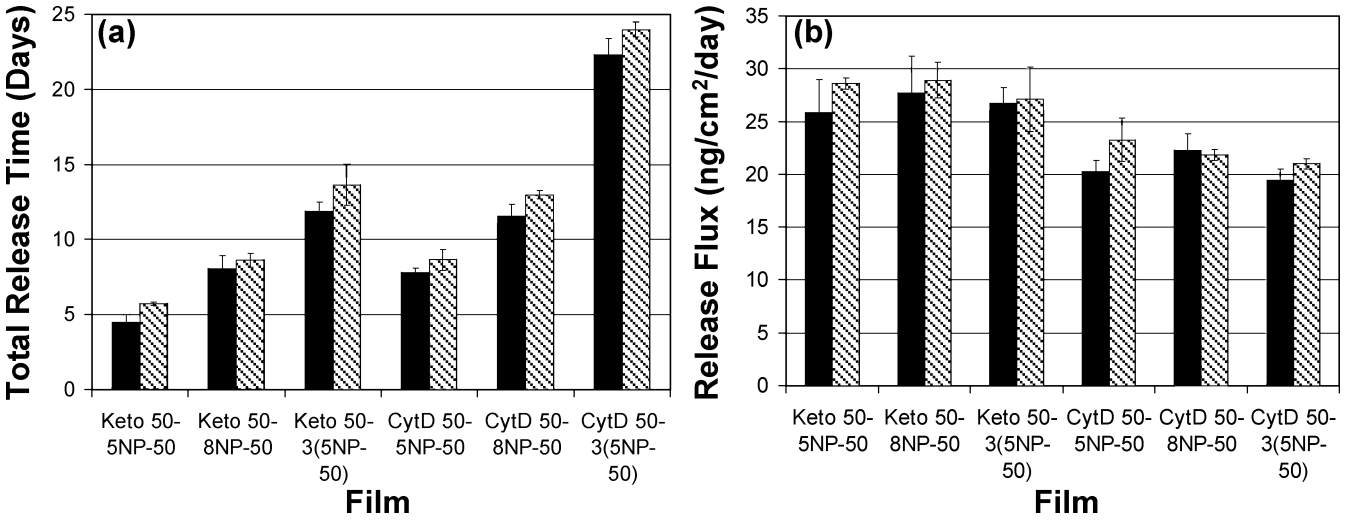

Figure 5. Graphs comparing the (a) total time to release and (b) release flux for ketoprofen and cytochalasin D at different loading concentrations. The solid bars are data from a film loaded with a 0.2 mg/mL DMSO loading solution, and the hatched bars are data from a film loaded with a 1.0 mg/mL solution for cytochalasin D and 10.0 mg/mL solution for ketoprofen.

drug release behavior of both homogeneous porous multilayers and multilayer heterostructures. These structural parameters included the number of porous bilayers, number of nonporous bilayers (in multilayer heterostructures), and the average pore size. We assume that the total amount released is a reasonable approximation of the amount of drug loaded in the films after the rinsing step. Two important trends are observed in Table 2 and Figure 5. The first trend is that the total time to release increases as the number of porous bilayers increases. The second is that the release flux only differs significantly when comparing nanoporous to microporous films. These trends will be discussed further in the next section.

Effect of Film Architecture on Release. By examining the results from the 8NP, 50-8NP-50, and 50-8NP-130 films, it can be concluded that the PAH/SPS nonporous layers have no significant effect on the drug release properties. For these three films, the total release time, release flux, and total amount released are statistically the same. This result is not surprising because small molecule drugs have been shown to have high mobility in nonporous polyelectrolyte multilayers in a buffered environment.[13,15] In previous reports, it was found that both PAH/PAA multilayers (nonporous) loaded with dye[15] and PAH/SPS multilayers built on drug particles[13] released the dye or drug molecules in a few minutes or less in a buffered environment. However, the nonporous film regions do have important properties that influence drug loading and release. In our experiments, they allow the drug solution to wick into the porous regions during the loading process if this technique is desired. Second, these results show that the nonporous regions do not inhibit the drug release when stacked on top of the porous regions. This characteristic could be useful in applications where functionalizing the surface is required for controlling interactions with biopolymers or cells. In addition, nonporous regions can be incorporated to make the films into dielectric mirrors that could be utilized as optical sensors.

The release flux did not change significantly when the number of porous layers was increased in films with a given magnitude of pore size (nanoporous or microporous). Comparing the full set of nanoporous films, 8NP, 15NP, 20NP, 50-5NP-50, 50-8NP-50, 50-8NP-130, and 50-3(5NP-50), Table 2 and Figure 5 show that most exhibit a similar release flux, approximately 27 $\pm$ 2 ng/cm^2/day for ketoprofen and 21 $\pm$ 3 ng/cm^2/day for cytochalasin D. The films with 15 and 20 nanoporous bilayers show a slight reduction in flux, perhaps due to the lower thickness per bilayer of the porous region in these films, which leads to a morphology change of the porous region. However, when the porous region is split by nonporous regions as in the case of the 50-3(5NP-50) films, the release flux is statistically the same as the 50-5NP-50 films.

For the nanoporous films, the total time to release the drug was directly proportional to the number of bilayers in the porous region(s). Figure 6 shows the total release time for each nanoporous system normalized by the number of bilayers in the porous region(s). Thus, the total release time is simply connected to the supply of drug in the nanoporous structure. Even if the porous region is split by a nonporous region, this proportionality holds, as apparent by the 50-3(5NP-50) film. For the nanoporous films, the average total release time is approximately 0.9 days/bilayer for ketoprofen and 1.5 days/bilayer for cytochalasin D. Because of this proportionality, longer release time periods than what is demonstrated in this study (approximately a month) are possible by increasing the number of porous bilayers in the film. However, this proportionality will be limited by the fact that uniform porosity transitions may not be possible for much thicker films.

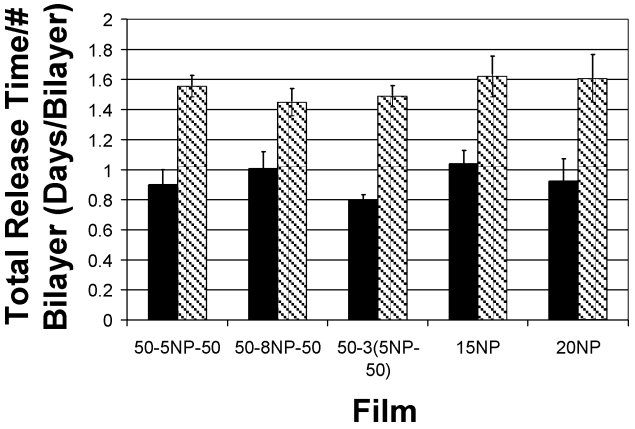

Figure 6. Total time of drug release normalized by the number of bilayers in the film. Drugs were loaded by absorption from a 0.2 mg/mL DMSO solution. Black bars represent total release time per bilayer for ketoprofen, and hatched bars represent total release time per bilayer for cytochalasin D.

As can be seen from these data, the total amount of released drug and the release flux are not drastically different for ketoprofen and cytochalasin D. Cytochalasin D does release somewhat slower and with a higher total amount released for all films in the study, but the difference is small considering the differences in structures and properties of the two drugs. Future work needs to be performed to elucidate the reasons for these subtle differences and determine the role that drug properties such as hydrophobicity and charge play in the release properties.

Release from Nanoporous versus Microporous Films. To gain a better understanding of the observed zero-order release kinetics exhibited by the nanoporous films, drug release from microporous multilayers was also investigated. The 15MP and 20MP films contained micropores of approximately 0.3−2.0 μm in diameter. It was demonstrated earlier (see Figure 4) that these microporous films released drugs at a faster rate than the corresponding nanoporous structures. In addition, the constant release rate (zero-order kinetics) of nanoporous films was not observed for the microporous films. This important pore-size-dependent difference in release mechanism is analyzed below.

The relative amount of drug released from both the microporous and the nanoporous films can be described using a model developed by Peppas et al.,[35]

$$\frac{M_t}{M_\infty} = kt^n \qquad (1)$$

where M_t is the total amount of drug released at time t, M_∞ is the total amount of drug released as time goes to infinity, k is a constant, and n is the exponent characteristic of the release mechanism. The value of n is equal to 1 for zero-order kinetics and is equal to 0.5 for Fickian diffusion. The drug release from the microporous films follows a Fickian diffusion mechanism. This is revealed in Figure 7a by how well the data fit to eq 1 (using least squares) with n as 0.5. In contrast, the nanoporous films followed zero-order release kinetics as observed in Figure 7b. In this case, the data were described well by eq 1 when n is set equal to 1. From this comparison, it is clear that the release mechanisms of microporous and nanoporous films are fundamentally different.

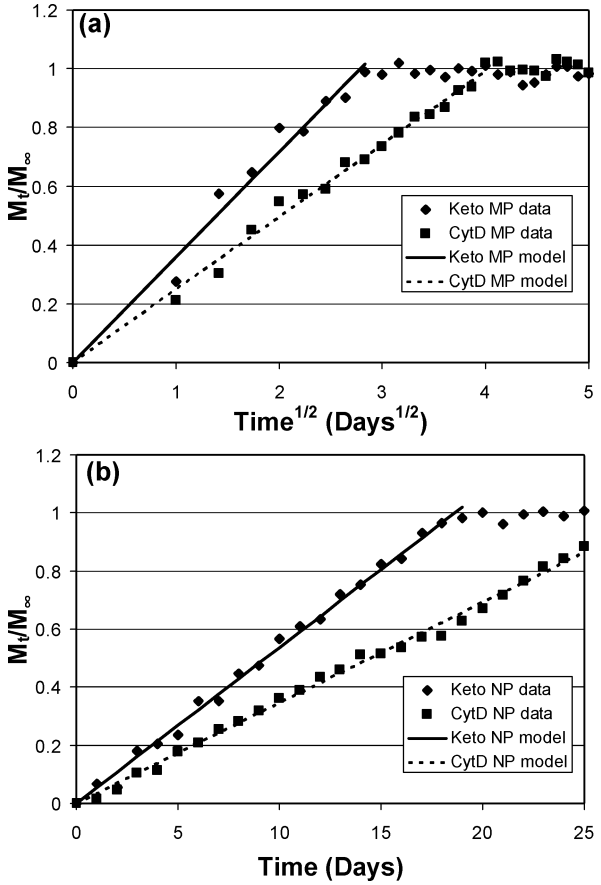

Figure 7. Comparison of ketoprofen and cytochalasin D release from (a) 20MP multilayers and (b) 20NP multilayers along with fitted curves from the model discussed in the text.

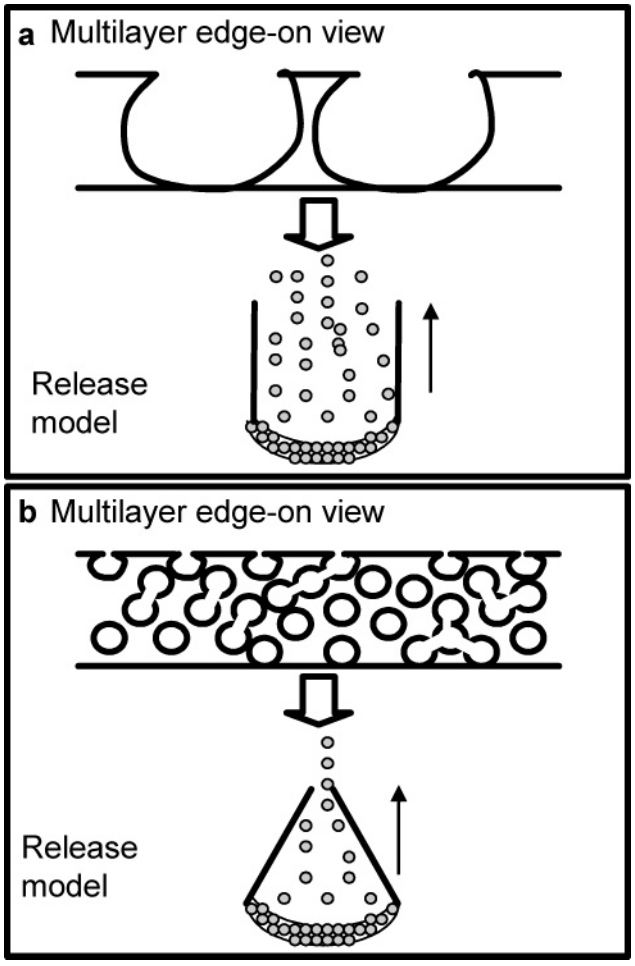

Figure 8. Schematic of porous multilayer films and implications on drug release for (a) microporous and (b) nanoporous films. The top drawing in each subsection represents an edge-on view of the multilayer, and the bottom drawing in each subsection compares conceptually the overall pore structure of a multilayer film to a single drug-containing vesicle.

The reason for zero-order release kinetics from nanoporous films, but not from microporous films, arises from differences in film morphology. The microporous and nanoporous film morphologies are represented schematically in Figure 8 to illustrate these differences. Micropores fill almost the entire thickness of the multilayer films and are very open to the surface. In contrast, only a small fraction of the pores are open to the surface in the nanoporous films. Because the micropores are open to the surface, the drug release follows Fickian behavior as it exits the pore. This phenomenon can be visualized as an open container where the molecules are free to diffuse into the continuous medium shown in Figure 8a. The nanopores present a much different release mechanism where drug must release from a few openings on the surface. These "defects" are very infrequent in number relative to the total supply of drug molecules, a situation known to favor zero-order release kinetics.[36,37] Inside the nanoporous films (submerged in buffer solution), transport of the drug molecules is fast. When a molecule of drug is released from one of the defects (a nanopore at the surface), it is replaced by another on a time scale that is fast as compared to the release mechanism. Thus, the observed release is dominated by the slower, defect-controlled zero-order mechanism. Brooke and Washkuhn modeled this effect using a geometric gradient with a large supply of drug as compared to a small opening for release.[38] This model, which captures the drug release behavior of nanoporous multilayers, is represented schematically in Figure 8b.

Cytochalasin D Release to Mammalian Cells. To demonstrate that a drug released from a nanoporous multilayer platform maintained its functionality, cytochalasin D was released into a culture of fibroblasts. Cytochalasin D inhibits cytoplasmic cleavage by blocking formation of contractile microfilaments resulting in multinucleated cells.[39] WT NR6 fibroblasts were grown on the surface of 50-5NP-50, 50-8NP-50, and 50-3(5NP-50) films with and without cytochalasin D loaded into the pores. In all cases, the influence of the cytochalasin D release could be easily seen in the change in the morphology of the fibroblasts. Figure 9 shows micrographs of fibroblasts on 50-3(5NP-50) films with DAPI stained nuclei. In the case of films loaded with cytochalasin D, the cells were multi-nucleated and had a much different morphology as compared to control samples (please see ref 9 for typical images of fibroblasts on various polyelectrolyte multilayer platforms and TCPS). This effect arises from the cells' inability to form actin stress fibers in the presence of cytochalasin D. The effect of the cytochalasin D release first became apparent approximately 2 days after cell seeding. The change in morphology and number of multi-nucleated cells increased on the third and fourth days before finally killing the cells. Cytochalasin D was also added directly to the cell culture media of fibroblasts seeded on tissue culture polystyrene at concentrations ranging from 100 to 1000 ng/mL (concentrations typical in cell biology experiments[39]) for comparison. The resulting morphology of cells exposed to 200−400 ng/mL cytochalasin D was similar to that shown in Figure 9. These results demonstrate that cytochalasin D is still functional after release from the porous multilayer film.

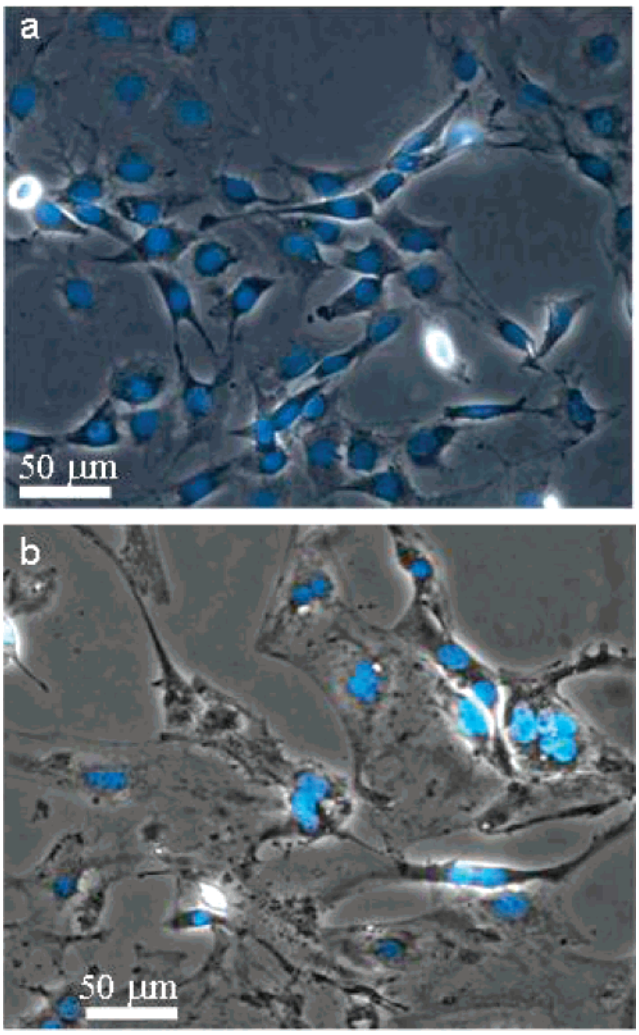

Figure 9. Microscope images of fibroblasts 3 days after seeding on 50-3(5NP-50) films with (a) no cytochalasin D and (b) cytochalasin D loaded from a 0.2 mg/mL DMSO solution. Nuclei were stained with DAPI.

Conclusions

We have developed porous polyelectrolyte multilayer ultrathin drug delivery systems in which the amount of drug loaded into the film along with the rate at which it is released can be controlled by changing structural parameters of the film. Ketoprofen and cytochalasin D were studied to represent different types of drugs that can be loaded and released from these multilayer films. The amount loaded and released could be tuned by varying the number of bilayers in the porous regions of films, and the release flux of a given drug could be controlled by varying the pore size. Microporous films released drug in accordance with Fickian diffusion, whereas the drugs loaded into nanoporous multilayers followed zero-order release kinetics. Incorporation of PAH/SPS nonporous layers in multilayer films had no distinguishable effect on the release behavior. However, the use of multilayer heterostructures that behaved as dielectric mirrors made it possible to monitor the drug loading.

Acknowledgment. This work was supported in part by the DuPont-MIT Alliance, the DARPA BOSS Program, and the MRSEC Program of the National Science Foundation under Award DMR 02-13282. We thank Prof. Paula T. Hammond and Dr. Geoff Lowman for helpful discussions, Shuguang Zhang and Carlos Semino for use of their cell culture facilities, the Institute of Soldier Nanotechnologies at MIT for use of their facilities for monitoring drug release, and Prof. James Sherley for helpful discussions about cytochalasin D.

References and Notes

(1) Langer, R. *Science* **1990**, *249*, 1527−1533.
(2) Babapulle, M. N.; Eisenberg, M. J. *Circulation* **2002**, *106*, 2734−2740.
(3) Babapulle, M. N.; Eisenberg, M. J. *Circulation* **2002**, *106*, 2859−2865.
(4) Salu, K. J.; Huang, Y. M.; Bosmans, J. M.; Liu, X. S.; Li, S. Q.; Wang, L.; Verbeken, E.; Bult, H.; Vrints, C. J.; De Scheerder, I. K. *Coron. Artery Dis.* **2003**, *14*, 545−555.
(5) Decher, G. *Science* **1997**, *277*, 1232−1237.
(6) Elbert, D. L.; Herbert, C. B.; Hubbell, J. A. *Langmuir* **1999**, *15*, 5355−5362.
(7) Serizawa, T.; Yamaguchi, M.; Matsuyama, T.; Akashi, M. *Biomacromolecules* **2000**, *1*, 306−309.
(8) Chluba, J.; Voegel, J. C.; Decher, G.; Erbacher, P.; Schaaf, P.; Ogier, J. *Biomacromolecules* **2001**, *2*, 800−805.
(9) Mendelsohn, J. D.; Yang, S. Y.; Hiller, J.; Hochbaum, A. I.; Rubner, M. F. *Biomacromolecules* **2003**, *4*, 96−106.
(10) Yang, S. Y.; Mendelsohn, J. D.; Rubner, M. F. *Biomacromolecules* **2003**, *4*, 987−994.
(11) Berg, M. C.; Yang, S. Y.; Hammond, P. T.; Rubner, M. F. *Langmuir* **2004**, *20*, 1362−1368.
(12) Caruso, F.; Trau, D.; Möhwald, H.; Renneberg, R. *Langmuir* **2000**, *16*, 1485−1488.
(13) Qiu, X.; Donath, E.; Möhwald, H. *Macromol. Mater. Eng.* **2001**, *286*, 591−597.
(14) Vazquez, E.; Dewitt, D. M.; Hammond, P. T.; Lynn, D. M. *J. Am. Chem. Soc.* **2002**, *124*, 13992−13993.
(15) Chung, A. J.; Rubner, M. F. *Langmuir* **2002**, *18*, 1176−1183.
(16) Quinn, J. F.; Caruso, F. *Langmuir* **2004**, *20*, 20−22.
(17) Burke, S. E.; Barrett, C. J. *Macromolecules* **2004**, *37*, 5375−5384.
(18) Nolan, C. M.; Serpe, M. J.; Lyon, L. A. *Biomacromolecules* **2004**, *5*, 1940−1946.
(19) Serpe, M. J.; Yarmey, K. A.; Nolan, C. M.; Lyon, L. A. *Biomacromolecules* **2005**, *6*, 408−413.
(20) Thierry, B.; Kujawa, P.; Tkaczyk, C.; Winnik, F. M.; Bilodeau, L.; Tabrizian, M. *J. Am. Chem. Soc.* **2005**, *127*, 1626−1627.
(21) Decher, G.; Lehr, B.; Lowack, K.; Lvov, Y.; Schmitt, J. *Biosens. Bioelectron.* **1994**, *9*, 677−684.
(22) Qiu, X.; Leporatti, S.; Donath, E.; Möhwald, H. *Langmuir* **2001**, *17*, 5375−5380.
(23) Zhang, J.; Chua, L. S.; Lynn, D. M. *Langmuir* **2004**, *20*, 8015−8021.
(24) Wood, K. C.; Boedicker, J. Q.; Lynn, D. M.; Hammond, P. T. *Langmuir* **2005**, *21*, 1603−1609.
(25) Thierry, B.; Winik, F. M.; Merhi, Y.; Silver, J.; Tabrizian, M. *Biomacromolecules* **2003**, *4*, 1564−1571.
(26) Li, Y. Y.; Cunin, F.; Link, J. R.; Gao, T.; Betts, R. E.; Reiver, S. H.; Chin, V.; Bhatia, S. N.; Sailor, M. J. *Science* **2003**, *299*, 2045−2047.
(27) Anglin, E. J.; Schwartz, M. P.; Ng, V. P.; Perelman, L. A.; Sailor, M. J. *Langmuir* **2004**, *20*, 11264−11269.
(28) Shiratori, S. S.; Rubner, M. F. *Macromolecules* **2000**, *33*, 4213−4219.
(29) Mendelsohn, J. D.; Barrett, C. J.; Chan, V. V.; Pal, A. J.; Mayes, A. M.; Rubner, M. F. *Langmuir* **2000**, *16*, 5017−5023.
(30) Hiller, J.; Mendelsohn, J. D.; Rubner, M. F. *Nat. Mater.* **2002**, *1*, 59−63.
(31) Zhai, L.; Nolte, A. J.; Cohen, R. E.; Rubner, M. F. *Macromolecules* **2004**, *37*, 6113−6123.
(32) Ahn, H.; Cohen, R. E.; Rubner, M. F. Unpublished work.
(33) Yoo, D.; Shiratori, S. S.; Rubner, M. F. *Macromolecules* **1998**, *31*, 4309−4318.
(34) Rafols, C.; Roses, M.; Bosch, E. *Anal. Chim. Acta* **1997**, *338*, 127−134.
(35) Ritger, P. L.; Peppas, N. A. *J. Controlled Release* **1987**, *5*, 23−36.
(36) Linsebigler, A. L.; Smentkowski, V. S.; Ellison, M. D.; Yates, J. T. *J. Am. Chem. Soc.* **1992**, *114*, 465−473.
(37) Kuznetsova, A.; Yates, J. T.; Liu, J.; Smalley, R. E. *J. Chem. Phys.* **2000**, *112*, 9590−9598.
(38) Brooke, D.; Wahkuhn, R. J. *J. Pharm. Sci.* **1977**, *66*, 159−162.
(39) Cooper, J. A. *J. Cell Biol.* **1987**, *105*, 1473−1478.

BM050174E